

Inhibitory Prodrug Approach for Selective Elimination of Immunosuppressive M2 Macrophages

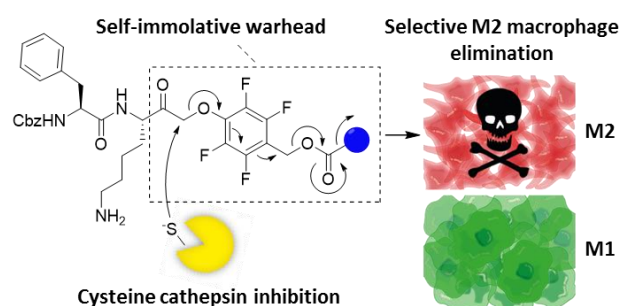
Floris J. van Dalen, Martijn Verdoes*

Department of Tumor Immunology and the Institute for Chemical Immunology, Radboud Institute for Molecular Life Sciences, Radboud University Medical Centre, Nijmegen, Netherlands

* Martijn.Verdoes@RadboudUMC.nl

Keywords: inhibitory prodrug, selective drug delivery, cysteine cathepsins, activity-based proteomics, tumor-associated macrophages, tumor microenvironment

Graphical Abstract



Abstract

Tumor associated macrophages (TAMs) support tumor development and have emerged as important regulators of therapeutic response to cytostatic agents. To target TAMs, we have developed a novel drug delivery approach which induces drug release in response to inhibition of pro-tumor cysteine cathepsin activity. Such inhibitory prodrug (IPD) establishes a self-regulated delivery system where drug release stops after all cysteine cathepsins are inhibited. This could improve the therapeutic window for drugs with severe side effects. We demonstrate this self-regulation concept with a fluorogenic IPD model. We have applied our IPD strategy to two cytotoxic agents, doxorubicin and monomethyl auristatin E, which could be efficiently released from the IPD scaffold to induce concentration dependent toxicity in RAW macrophages. Lastly, by taking advantage of the increased cathepsin activity in TAM-like M2 polarized bone marrow derived macrophages, we show that IPD Dox selectively eliminates M2 over M1 macrophages. This demonstrates the potential of our IPD strategy for selective drug delivery and modulation of the tumor microenvironment.

Main text

Chemotherapy remains the first line of defense against cancer. However, most anticancer drugs suffer from dose-limiting adverse effects. For instance, the use of doxorubicin is restricted by dose-accumulating cardiotoxicity.^{1,2} Selective delivery of cytotoxic drugs is an attractive strategy to improve the therapeutic window. Substrate prodrugs employ tumor-overexpressed enzymes to locally trigger drug activation. Cysteine cathepsins (cCTSs) are highly upregulated in cancer and support tumor development in all stages of disease.³ cCTSs cleave the extracellular matrix and cell adherence molecules paving the way for invading tumor cells.³⁻⁷

Moreover, they are involved in activating growth factors and angiogenesis.^{3,8,9} In the tumor microenvironment (TME), cCTS activity is predominantly localized in tumor-associated macrophages (TAMs).^{10,11} TAMs can make up a significant portion of the tumor mass (up to >30%) and support tumor development into malignancy.^{12,13} They display an M2-like phenotype, hallmarked by immunosuppressive factors (e.g. interleukin 10, programmed death ligand 1, transforming growth factor beta), increased excretion of angiogenic molecules (e.g. adrenomedullin and vascular epithelial growth factors) and an increase in matrix metalloprotease- and cCTS-activity.¹⁴ TAMs have emerged as important regulators of therapeutic response to cytostatic agents and present an immunosuppressive barrier for effector functions of T lymphocytes and NK cells.¹²⁻¹⁴ Therefore, cCTS activity in TAMs presents an attractive target for cancer treatment.

Several cathepsin-targeted prodrugs have been developed aimed at selective delivery to the TME.¹⁵⁻¹⁸ However, these approaches allow cCTS-activity to continue along with the associated tumor-promoting processes. Inhibition of cCTSs has been demonstrated to reduce tumor malignancy in preclinical models and exhibits synergistic effects with cytostatic agents such as cyclophosphamide and doxorubicin.^{19,20} Therefore, we designed a single molecule prodrug approach that simultaneously inhibits cCTSs as it induces drug release, through the development of a self-immolative warhead (figure 1). This design, dubbed inhibitory prodrug (IPD), establishes a self-regulated system where drug release stops after all cCTSs are inhibited. This will potentially broaden the therapeutic window for drugs with severe side effects. Furthermore, this form of drug delivery could intrinsically synergize cCTS inhibition and cytotoxic agents by targeting TAMs in two distinct manners. That is, invasion, metastasis and angiogenesis are reduced by cCTS inhibition, after which the cytotoxic agent can eliminate immunosuppressive TAMs and could potentially kill adjacent tumor cells through the bystander effect.

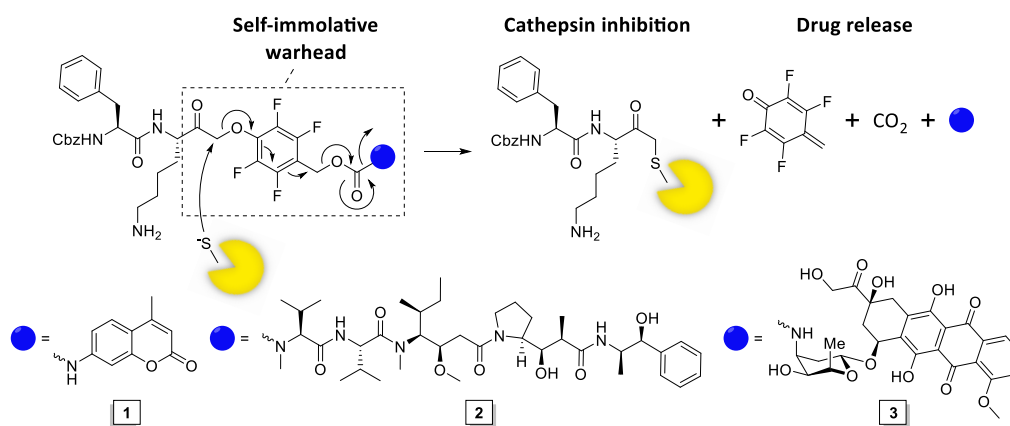


Figure 1. The mechanism of action of the self-immolative warhead and structures of IPD-AMC (1), IPD-MMAE (2), and IPD-Dox (3). In short, nucleophilic attack on the phenoxymethyl ketone results in cathepsin inhibition followed by self-immolation and payload release.

As a proof-of-concept we designed and synthesized a model IPD (1, IPD-AMC) containing a latent fluorophore, 7-amino-4-methylcoumarin (AMC) (Figures 1 and Scheme S1). This fluorophore remains quenched until it is released from the IPD, with a quenching efficiency of >99% for intact IPD-AMC (Figure S2A). To examine the inhibitory potency we performed a competitive activity-based protein profiling (cABPP) experiment in which intact RAW 264.7 macrophages (mouse monocytic leukemic macrophage cell line) or RAW lysate were treated with a titration of IPD-AMC and the residual cathepsin activity was determined with pan-reactive probe BMV109 (Figure 2A).¹⁰ This demonstrated complete cathepsin inhibition at approximately 1 μ M IPD-AMC in both lysate and live cells, which is in the same order of magnitude as the pentafluoro-phenoxymethyl ketone (PMK) inhibitor FJD005 (Figure S7). This shows that IPD-AMC is efficiently internalized by cells and that attachment of the

molecular cargo at the prime site does not interfere with cathepsin binding. To determine whether this inhibition also resulted in release of the fluorogenic cargo, we measured fluorogenic activation of AMC upon exposure of RAW lysate to 2.5 μM IPD-AMC for 1 hour (Figure 2B). This produced AMC fluorescence corresponding to some 50 nM (~ 15 AU), which was reduced to background levels either by denaturing the proteins in the lysate or by pretreatment with cathepsin inhibitor FJD005, indicating that AMC release is controlled by cathepsin activity. Because cargo release proceeds in two steps (nucleophilic displacement of the phenol by the active-site cysteine, followed by self-immolation and AMC release), we investigated the correlation between cCTS inhibition- and AMC fluorescent activation-kinetics with a tandem cABPP and AMC release experiment (Figures 2C and S2F). This demonstrated that AMC activation and cathepsin inhibition both plateau after 30 min, indicating that AMC is released in a concerted action upon target inhibition (at the investigated time-scale). This assures that drug activation will remain localized in cells or environments with high cathepsin activity. This AMC release plateau is stable for over 6 hours, confirming the stability of the IPD (Figure S2D).

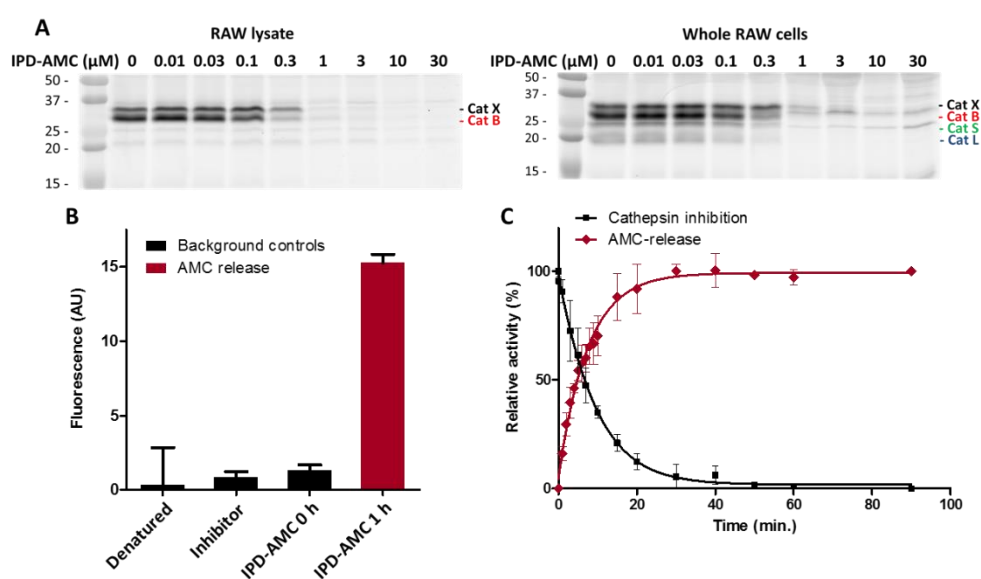


Figure 2. Cathepsin inhibition and AMC release by IPC-AMC. **A)** RAW lysate (corresponding to 2×10^5 cells) or live RAW cells (2×10^5 cells) were incubated with indicated concentration of IPD-AMC (1 h, 37°C) after which residual cathepsin activity was labeled with BMV109 ($1 \mu\text{M}$, 1 h, 37°C). Cells were lysed and proteomes were separated by SDS PAGE. Cathepsin labeling was visualized by in-gel fluorescence scanning. **B)** AMC release from IPD-AMC ($2.5 \mu\text{M}$) in RAW lysate is blocked after deactivating the lysate by denaturation (5 min, 95°C) or inhibition of cCTSs by inhibitor FJD005 ($10 \mu\text{M}$, 5 min, 37°C) ($n = 3$). **C)** AMC release correlates with cathepsin inhibition over time as determined by in tandem competitive labeling with BMV109. This indicates immediate AMC release following cathepsin inhibition at the observed time-scale ($n = 3$).

An important consequence of our IPD design is the release of equimolar amounts of drug cargo relative to the concentration of active cCTSs. Therefore, the inherent toxicity of the payload needs to be carefully considered to obtain the required IPD potency and selectivity. We chose two cytotoxic drugs with different toxicities: monomethyl auristatin E (MMAE) with 1-10 nanomolar toxicity and doxorubicin (Dox) in the 10-100 nanomolar range. We synthesized the corresponding IPD-MMAE (**2**) and IPD-Dox (**3**) (Figure 1 and Scheme S2). Subsequent competitive labelling in live RAW macrophages demonstrated similar inhibitory potency as IPD-AMC (Figure 3A). To measure IPD toxicity we treated RAWs with cytostatic agents or corresponding IPDs for three days and assayed cell viability with an MTT assay (Figure 3B,C). This resulted in a half-maximal effective concentration (EC_{50}) of 7.3 nM for MMAE and 43 nM for Dox, where the IPDs displayed efficient activation for both cytotoxic payloads, namely 32 nM and 125 nM for IPD-MMAE and IPD-Dox, respectively (Figure 3B,C and Table S1). This 3-fold reduction in toxicity is probably a result of the inhibitory nature of the delivery system, where payload

release is directly coupled to the concentration of active cathepsins. To determine whether toxicity is dependent on drug activation, we synthesized a control IPD (IPD-Ctrl), containing a non-immolative PMK warhead to prevent the release of active Dox (Figure S4 and Scheme S3). This indeed increased the EC50 in RAW macrophages two orders of magnitude (to >10 μ M, Figure 3C).

Subsequently, we attempted to determine the cathepsin dependency of IPD toxicity by inhibiting cCTSs prior to treatment, by preincubation with FJD005. However, this preinhibition could not rescue cell viability (Figure S5). Instead, we noticed sensitization to further treatment, indicating possible synergy between the PMK warhead and cytotoxic agents. This sensitization by FJD005 might be the result of NPLR3 inflammasome activation through inhibition of GAPDH or α -enolase as described by Sanman et al.²² To avoid these potential off-target effects we next tried preinhibition with epoxysuccinate WL898 (reported as R14Et).²¹ However, this had no noticeable effect on IPD toxicity (Figure S6). To explain this unaltered toxicity, we looked at the dynamics of cathepsin activity following preinhibition, by labeling with BMV109 (Figure S7). This revealed that soon after initial inhibition, replenishment of cathepsin activity is apparent and complete recovery is observed after 24 hours. In an attempt to counter this replenished cathepsin activity we added WL898 every 8 hours. This still did not alter the toxicity profile of the IPDs (Figure S8). When we labelled the cathepsin activity under these optimized conditions, we again see a replenishment of cathepsin activity within 24 hours, albeit reduced to about 10% of baseline activity (Figure S9). Whether this recurring cathepsin activity is responsible for the largely unaltered toxicity profile is difficult to conclude. Interestingly, target preinhibition toxicity experiments are rarely reported in prodrug literature. Instead, other control experiments are performed (Table S2). This might suggest that sustained on-target inhibition is difficult to attain. Alternatively, the cytotoxic agent could be released by off-target activity (not detectable with BMV109) or the IPD is unstable in the cell culture conditions. To exclude the latter, we assayed IPD stability in serum-containing medium at 37 °C, which displayed >95% stability for all three IPDs up to 72 hours (Figure S10).

The most commonly reported validation of targeted drug release is the comparison of induced toxicity between cell types with differential cCTS expression. As outlined above, the majority of cCTS activity in the TME is localized in TAMs with an M2-like phenotype.^{10,11} When we compared cathepsin activity in M1- and M2-polarized mouse bone marrow-derived macrophages (BMDMs) *in vitro*, M2s have a two-fold cCTS activity compared to M1s (Figure 3D and Figure S11). Thus, we exposed M1 and M2 BMDMs to cytotoxic drugs or IPDs and established EC50s with an MTT assay (Figure 3E). This revealed that M2 macrophages are 4.6-fold more sensitive to Dox alone compared to M1s (EC50: M2 = 86 nM vs M1 = 392 nM). As observed in RAW macrophages (Figure 3C), the toxicity of IPD-Dox in M2s was reduced some 3-fold relative to free Dox. This reduction in toxicity was more than 10-fold for M1 BMDMs, increasing IPD-Dox selectivity for M2s to about 18-fold (EC50: M2 = 229 nM vs M1 = 4.17 μ M). Moreover, the increased cathepsin activity in M2s creates a selectivity window between M2 and M1 BMDMs, as IPD-Dox can selectively eliminate M2 macrophages at 1 μ M, while Dox alone hits both M2 and M1 at this concentration (Figure 3F). Because LPS-treated M1 macrophages are reported to have an increased activity of α -enolase and GAPDH (two possible off-targets of the PMK warhead) compared to M2 macrophages,^{22,24,25} this cannot explain the observed selectivity window. Thus, taken together we conclude that the predominant mechanism of action of IPD-Dox selectivity for M2 macrophages is due to the increased cathepsin activity compared to M1 macrophages. MMAE only displays a limited response in BMDMs, with M2s being more sensitive to MMAE and IPD-MMAE (Figure S12). As MMAE is strictly antimetabolic, through inhibition of tubulin polymerization, it has limited activity in non-proliferating cells, such as terminally differentiated primary cells.

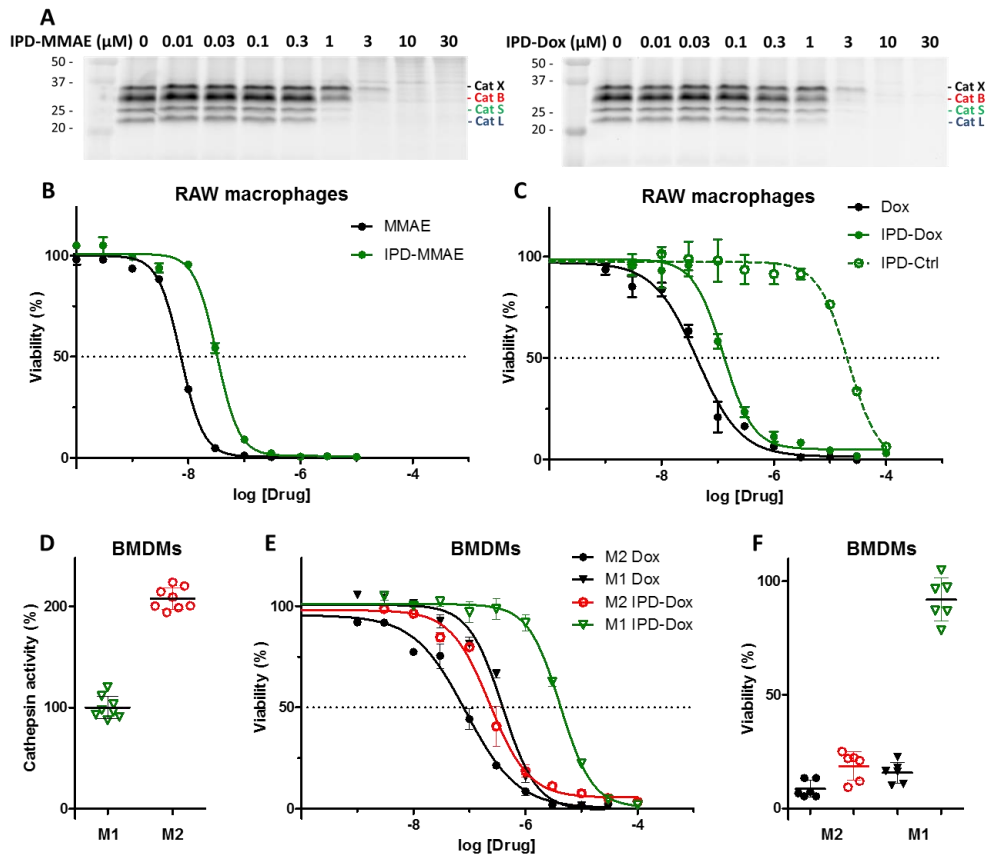


Figure 3. Inhibitory profile and cell killing of cytotoxic IPDs IPD-MMAE and IPD-Dox. **A)** Live RAW cells were incubated with indicated concentration of IPD-MMAE and IPD-Dox (1 h, 37 °C), followed by labeling with BMV109 (1 μM, 1 h, 37 °C). Proteomes were separated by SDS PAGE and visualized by in-gel fluorescence scanning (n=2). **B, C)** RAWs were treated with indicated concentration of cytostatic drug or IPD for 3 days, after which cell viability was assessed by MTT assay (N=3, n=2). **D)** Bone marrow-derived macrophages were polarized into M1 or M2 subsets and relative cathepsin activity was determined by labeling with BMV109 (1 μM, 1h, 37 °C) (n=6). **E)** M1 and M2 BMDMs were treated with indicated concentrations of doxorubicin or IPD-Dox for 3 days, after which cell viability was assessed by MTT assay. M2 macrophages display higher sensitivity toward doxorubicin (some 4-fold) compared to M1 macrophages and IPD-mediated delivery increases this selectivity (some 18-fold) (n=6). **F)** M2-selective killing can be achieved at 1 μM concentration in vitro (n=6).

In conclusion, we have designed a novel self-limiting IPD strategy to simultaneously inhibit cathepsin activity and direct drug release to cells or environments with high cathepsin activity. The designed IPDs show effective release in *in vitro* models, whereas a warhead in which the leaving group is a non-immolative Dox conjugate rescues cell viability. Lastly, by leveraging the increased cathepsin activity in TAM-like M2-polarized BMDMs, we show that this strategy allows selective elimination of M2 over M1 macrophages. This drug delivery approach could be expanded to other cysteine proteases by substitution of the dipeptide target recognition motif. Switching the payload to small molecule immunostimulants could facilitate repolarization of TAMs into an anti-tumor M1-like state. Together, our results demonstrate the potential of the IPD strategy for modulation of the immunosuppressive TME.

- (1) Chatterjee, K.; Zhang, J.; Honbo, N.; Karliner, J. S. Doxorubicin Cardiomyopathy. *Cardiology* **2010**, *115* (2), 155–162. <https://doi.org/10.1159/000265166>.
- (2) Tacar, O.; Sriamornsak, P.; Dass, C. R. Doxorubicin: An Update on Anticancer Molecular Action, Toxicity and Novel Drug Delivery Systems. *J. Pharm. Pharmacol.* **2013**, *65* (2), 157–170. <https://doi.org/10.1111/j.2042-7158.2012.01567.x>.
- (3) Olson, O. C.; Joyce, J. A. Cysteine Cathepsin Proteases: Regulators of Cancer Progression and Therapeutic Response. *Nat. Rev. Cancer* **2015**, *15* (12), 712–729. <https://doi.org/10.1038/nrc4027>.
- (4) Mai, J.; Sameni, M.; Mikkelsen, T.; Sloane, B. F. Degradation of Extracellular Matrix Protein Tenascin-C by Cathepsin B: An Interaction Involved in the Progression of Gliomas. *Biol. Chem.* **2005**, *383* (9), 1407–1413. <https://doi.org/10.1515/BC.2002.159>.
- (5) Gocheva, V.; Wang, H.-W.; Gadea, B. B.; Shree, T.; Hunter, K. E.; Garfall, A. L.; Berman, T.; Joyce, J. A. IL-4 Induces Cathepsin Protease Activity in Tumor-Associated Macrophages to Promote Cancer Growth and Invasion. *Genes Dev.* **2010**, *24* (3), 241–255. <https://doi.org/10.1101/gad.1874010>.
- (6) Sevenich, L.; Bowman, R. L.; Mason, S. D.; Quail, D. F.; Rapaport, F.; Elie, B. T.; Brogi, E.; Brastianos, P. K.; Hahn, W. C.; Holsinger, L. J.; Massagué, J.; Leslie, C. S.; Joyce, J. A. Analysis of Tumor- and Stroma-Supplied Proteolytic Networks Reveals a Brain Metastasis-Promoting Role for Cathepsin S. *Nat. Cell Biol.* **2014**, *16* (9), 876–888. <https://doi.org/10.1038/ncb3011>.
- (7) Sobotič, B.; Vizovišek, M.; Vidmar, R.; Van Damme, P.; Gocheva, V.; Joyce, J. A.; Gevaert, K.; Turk, V.; Turk, B.; Fonović, M. Proteomic Identification of Cysteine Cathepsin Substrates Shed from the Surface of Cancer Cells. *Mol. Cell. Proteomics MCP* **2015**, *14* (8), 2213–2228. <https://doi.org/10.1074/mcp.M114.044628>.
- (8) Wang, B.; Sun, J.; Kitamoto, S.; Yang, M.; Grubb, A.; Chapman, H. A.; Kalluri, R.; Shi, G.-P. Cathepsin S Controls Angiogenesis and Tumor Growth via Matrix-Derived Angiogenic Factors. *J. Biol. Chem.* **2006**, *281* (9), 6020–6029. <https://doi.org/10.1074/jbc.M509134200>.
- (9) Small, D. M.; Burden, R. E.; Jaworski, J.; Hegarty, S. M.; Spence, S.; Burrows, J. F.; McFarlane, C.; Kissenpfennig, A.; McCarthy, H. O.; Johnston, J. A.; Walker, B.; Scott, C. J. Cathepsin S from Both Tumor and Tumor-Associated Cells Promote Cancer Growth and Neovascularization. *Int. J. Cancer* **2013**, *133* (9), 2102–2112. <https://doi.org/10.1002/ijc.28238>.
- (10) Verdoes, M.; Oresic Bender, K.; Segal, E.; van der Linden, W. A.; Syed, S.; Withana, N. P.; Sanman, L. E.; Bogyo, M. Improved Quenched Fluorescent Probe for Imaging of Cysteine Cathepsin Activity. *J. Am. Chem. Soc.* **2013**, *135* (39), 14726–14730. <https://doi.org/10.1021/ja4056068>.
- (11) Jakoš, T.; Pišlar, A.; Jewett, A.; Kos, J. Cysteine Cathepsins in Tumor-Associated Immune Cells. *Front. Immunol.* **2019**, *10*. <https://doi.org/10.3389/fimmu.2019.02037>.
- (12) Qian, B.-Z.; Pollard, J. W. Macrophage Diversity Enhances Tumor Progression and Metastasis. *Cell* **2010**, *141* (1), 39–51. <https://doi.org/10.1016/j.cell.2010.03.014>.
- (13) Olson, O. C.; Kim, H.; Quail, D. F.; Foley, E. A.; Joyce, J. A. Tumor-Associated Macrophages Suppress the Cytotoxic Activity of Antimitotic Agents. *Cell Rep.* **2017**, *19* (1), 101–113. <https://doi.org/10.1016/j.celrep.2017.03.038>.
- (14) Van Dalen, F. J.; Van Stevendaal, M. H. M. E.; Fennemann, F. L.; Verdoes, M.; Ilina, O. Molecular Repolarisation of Tumour-Associated Macrophages. *Molecules* **2019**, *24* (1), 9. <https://doi.org/10.3390/molecules24010009>.
- (15) Dubowchik, G. M.; Mosure, K.; Knipe, J. O.; Firestone, R. A. Cathepsin B-Sensitive Dipeptide Prodrugs. 2. Models of Anticancer Drugs Paclitaxel (Taxol®), Mitomycin C and Doxorubicin. *Bioorg. Med. Chem. Lett.* **1998**, *8* (23), 3347–3352. [https://doi.org/10.1016/S0960-894X\(98\)00610-6](https://doi.org/10.1016/S0960-894X(98)00610-6).
- (16) Moon, S.-J.; Govindan, S. V.; Cardillo, T. M.; D'Souza, C. A.; Hansen, H. J.; Goldenberg, D. M. Antibody Conjugates of 7-Ethyl-10-Hydroxycamptothecin (SN-38) for Targeted Cancer Chemotherapy. *J. Med. Chem.* **2008**, *51* (21), 6916–6926. <https://doi.org/10.1021/jm800719t>.
- (17) Zhang, X.; Tang, K.; Wang, H.; Liu, Y.; Bao, B.; Fang, Y.; Zhang, X.; Lu, W. Design, Synthesis, and Biological Evaluation of New Cathepsin B-Sensitive Camptothecin Nanoparticles Equipped with a Novel Multifunctional Linker. *Bioconjug. Chem.* **2016**, *27* (5), 1267–1275. <https://doi.org/10.1021/acs.bioconjchem.6b00099>.
- (18) Karthaler-Benbakka, C.; Koblmüller, B.; Mathuber, M.; Holste, K.; Berger, W.; Heffeter, P.; Kowol, C. R.; Keppler, B. K. Synthesis, Characterization and in Vitro Studies of a Cathepsin B-Cleavable Prodrug of the VEGFR Inhibitor Sunitinib. *Chem. Biodivers.* **2019**, *16* (1). <https://doi.org/10.1002/cbdv.201800520>.
- (19) Bell-McGuinn, K. M.; Garfall, A. L.; Bogyo, M.; Hanahan, D.; Joyce, J. A. Inhibition of Cysteine Cathepsin Protease Activity Enhances Chemotherapy Regimens by Decreasing Tumor Growth and Invasiveness in a Mouse Model of Multistage Cancer. *Cancer Res.* **2007**, *67* (15), 7378–7385. <https://doi.org/10.1158/0008-5472.CAN-07-0602>.
- (20) Gangoda, L.; Keerthikumar, S.; Fonseka, P.; Edgington, L. E.; Ang, C.-S.; Ozcitti, C.; Bogyo, M.; Parker, B. S.; Mathivanan, S. Inhibition of Cathepsin Proteases Attenuates Migration and Sensitizes Aggressive N-Myc Amplified Human Neuroblastoma Cells to Doxorubicin. *Oncotarget* **2015**, *6* (13), 11175–11190. <https://doi.org/10.18632/oncotarget.3579>.
- (21) van der Linden, W. A.; Schulze, C. J.; Herbert, A. S.; Krause, T. B.; Wirchnianski, A. A.; Dye, J. M.; Chandran, K.; Bogyo, M. Cysteine Cathepsin Inhibitors as Anti-Ebola Agents. *ACS Infect. Dis.* **2016**, *2* (3), 173–179. <https://doi.org/10.1021/acsinfecdis.5b00130>.
- (22) Sanman, L. E.; Qian, Y.; Eisele, N. A.; Ng, T. M.; van der Linden, W. A.; Monack, D. M.; Weerapana, E.; Bogyo, M. Disruption of Glycolytic Flux Is a Signal for Inflammasome Signaling and Pyroptotic Cell Death. *eLife* **2016**, *5*. <https://doi.org/10.7554/eLife.13663>.
- (23) Mata, G.; do Rosário, V. E.; Iley, J.; Constantino, L.; Moreira, R. A Carbamate-Based Approach to Primaquine Prodrugs: Antimalarial Activity, Chemical Stability and Enzymatic Activation. *Bioorg. Med. Chem.* **2012**, *20* (2), 886–892. <https://doi.org/10.1016/j.bmc.2011.11.059>.
- (24) Reales-Calderón, J. A.; Aguilera-Montilla, N.; Corbí, Á. L.; Molero, G.; Gil, C. Proteomic Characterization of Human Proinflammatory M1 and Anti-Inflammatory M2 Macrophages and Their Response to *Candida Albicans*. *PROTEOMICS* **2014**, *14* (12), 1503–1518. <https://doi.org/https://doi.org/10.1002/pmic.201300508>.
- (25) Liu, Y.; Xu, R.; Gu, H.; Zhang, E.; Qu, J.; Cao, W.; Huang, X.; Yan, H.; He, J.; Cai, Z. Metabolic Reprogramming in Macrophage Responses. *Biomark. Res.* **2021**, *9* (1), 1. <https://doi.org/10.1186/s40364-020-00251-y>.